Electron irradiation-induced defects in Mo-diluted FeCrNi austenitic alloy during void swelling incubation

B Y Wang[1], E Y Lu[1], C X Zhang[1], Q Xu[2], S X Jin[1], P Zhang[1], X Z Cao[1,*]

[1] Key Laboratory of Nuclear Radiation and Nuclear Energy Technology, Institute of High Energy Physics, CAS, Beijing, 100049, China

[2] Research Reactor Institute, Kyoto University, Kumatori-cho, Osaka 590-0494, Japan

E-mail: caoxzh@ihep.ac.cn

Abstract. The microstructural features and the effect of Mo addition during incubation period in FeCrNi austenitic alloy were investigated using positron annihilation technique and micro-Vickers Hardness. The electron irradiation, which could induce vacancy defects in material, was performed at room temperature up to the dose of 1.7×10^{-4} and 5×10^{-4} dpa, respectively. The defect concentration was estimated about 10^{-4}-10^{-7} though standard trapping model. The added Mo could trap vacancies to form Mo-vacancy complexes, which may suppress the migration and growth of vacancy defects during electron irradiation. In addition, the microstructural evolution during electron radiation resulted in hardening, while the added Mo might to improve the hardening property of the alloy.

1. Introduction

Austenitic stainless steels are usually used as the structural material of nuclear reactors. Irradiation damage, such as void swelling and hardening, caused by prolonged energetic particle irradiation may affect the safety of nuclear reactors [1-2]. A transient stage or incubation period, which could determine the duration of the nuclear system, exists before steady void swelling occurs. Several theoretical and experimental analyses have been performed on the microstructural evolution during the incubation period [3-6]. It is difficult to characterize the micro defects in this period by TEM for the reason that the defect size was usually lower than the resolution limit of TEM. Positron Annihilation Technique (PAT) is a suitable method to detect defects, which are below the resolution limit of TEM. It is known that the defect structures of the incubation period related with the irradiation temperature and dose. No microvoids would be found for the irradiation temperature above 473 K with the dose of 10^{-3} dpa in neutron irradiated Ti-modified 316SS [7-8]. Meanwhile, the alloy elements may also affect the defect structures during the incubation period [1-2, 9-10]. As reported, undersize impurity atoms (P, Si) interact with interstitial atoms, while oversized impurities (Ti, Nb) would interact with vacancies under irradiation in austenitic alloy [2]. These minor elements might induce the formation of stacking fault tetrahedral and precipitates but prevent the void growth [1, 9]. The added Mo could trap impurity atoms and reduce the number of dislocation loops under irradiation [10]. Additionally, Mo addition could affect the formation of precipitates and crystal texture then enhanced the mechanical properties and corrosion behaviour in different alloys [11-14]. As we know, the added Mo is the essential atoms in FeCrNi austenitic stainless steel. However, few studies were performed on the interaction of Mo addition with vacancy defects during incubation period.

In this study, FeCrNi and Mo-diluted model alloys were used to avoid the effect of other impurity elements. Electron irradiation was performed to generate vacancy defects. PATs, including Positron annihilation lifetime spectroscopy (PALS), Doppler broadening spectroscopy (DBS) and coincidence Doppler broadening (CDB), were used to investigate the microstructural evolution under electron irradiation and the effect of Mo addition on microstructures. Irradiation hardening was characterized by micro-Vickers Hardness.

2. Experimental details

FeCrNi alloy (17wt% Cr, 12wt% Ni, the balance Fe) and Mo-diluted alloy (17wt% Cr, 12wt% Ni, 2.2wt% Mo, the balance Fe) were made from a series of high purity metals (≥4N) by arc melting process at General Research Institute for Nonferrous Metals. Specimens with the size of 10×10×0.3 mm were electron-chemical polished to have a mirror like surface, and then annealed at 1323 K for 2 h in vacuum (about 1×10^{-4} Pa).

Electron irradiation was performed by an electron linear accelerator of Research Reactor Institute, Kyoto University with an acceleration voltage of 8 MV at less than 373 K. The damage rate was about 8×10^{-8} dpa/s and the irradiation dose was 1.7×10^{-4} dpa and 5×10^{-4} dpa, respectively.

PATs were performed to characterize the microstructural evolution of irradiated alloy at room temperature. PALS were carried out by a conventional fast-slow spectrometer with a time resolution of 197 ps (FWHM). In order to reduce the statistical error, each spectrum accumulated about 2×10^{6} coincidence events within 2 h. The spectra were decomposed into two components (τ_1 and τ_2) by LT9 after subtracting the source component and background. DBS were performed with a high purity germanium detector. The S parameter was defined as the ratio counts in the central energy region (511±0.76 keV) to the total counts of the spectrum (511±7.66 keV). CDB were performed to identify the chemical elements with two high purity germanium detectors placed 180° [15-16]. Each CDB spectrum was accumulated to 1×10^{7} counts to reduce the statistical error. Additionally, micro-Vickers Hardness was performed for all specimens with different irradiation condition.

3. Results and discussion

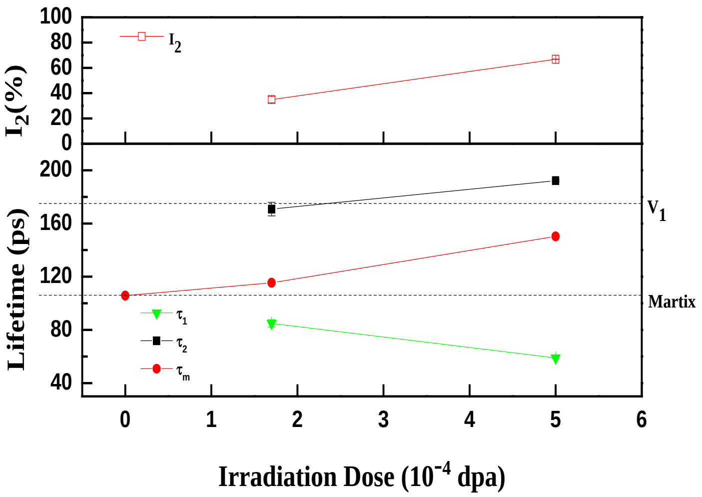

Figure 1. Dose dependence of the positron annihilation lifetime for electron irradiated FeCrNi model alloy.

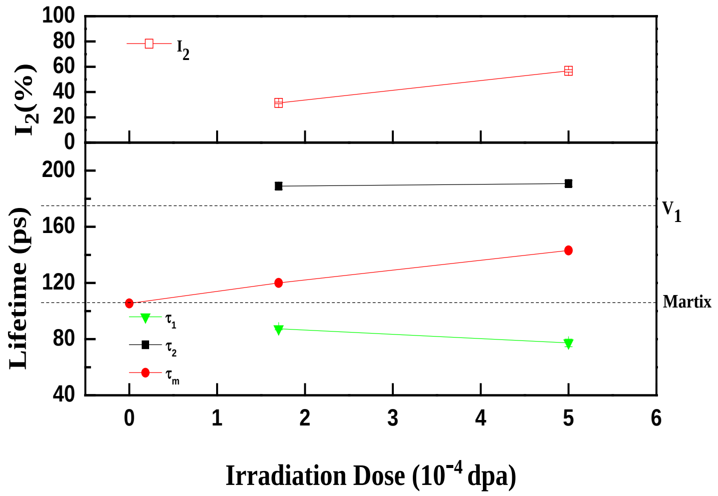

Figure 2. Dose dependence of the positron annihilation lifetime for electron irradiated Mo-diluted alloy.

Figure 1 and Figure 2 plot the dose dependence of the positron annihilation lifetime for electron irradiated FeCrNi and Mo-diluted alloy, respectively. τ_1, τ_2 and τ_m denoted the short, long and mean positron lifetimes, respectively. I_2 denoted the long lifetime intensity. The calculated lifetimes of matrix, mono-vacancy (V_1) and di-vacancy (V_2) of Ni are 106, 175 and 195 ps, respectively [8]. The mean lifetimes for both unirradiated alloys are about 105 ps, which is similar to the matrix value of Ni [8]. In Figure 1, the long lifetime at low irradiation dose is 171 ± 5.1 ps, which is accord with the calculated mono-vacancy value (V_1). The result of higher irradiation dose is 189±5.1 ps, which is larger than V_1 but smaller than V_2. These results indicate that certain amount of small-sized vacancy defects generated after electron irradiation. The increment of I_2 for both alloys indicates much more vacancy defects generated with elevated irradiation dose. However, I_2 in Mo-diluted alloy are slightly lower than that in FeCrNi alloy at the same irradiation condition. The added Mo might suppress the generation of vacancy defects during electron irradiation.

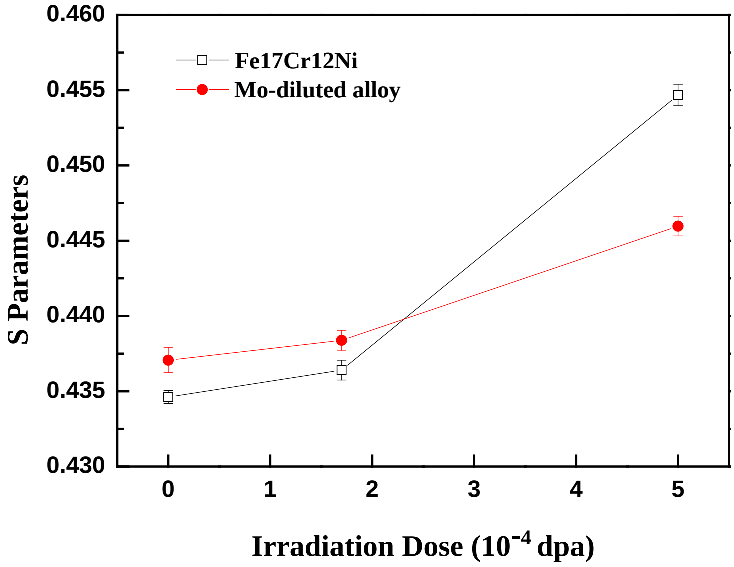

Figure 3. Dose dependence of S parameter for FeCrNi and Mo-diluted alloy.

Figure 3 shows the S parameters of both alloys irradiated with different dose. The values of unirradiated alloys attributed from the positron annihilated in matrix. The S parameters for both model alloys increased obviously with increasing irradiation dose, which means the increment of the defect concentration. The variation trend of S parameter for FeCrNi increased more sharply than that in Mo-diluted alloy, which means less defects generated in Mo-diluted alloy. According to the standard trapping model (STM) [17], the concentration of mono-vacancies can be estimated as:

$$C_V = \frac{\lambda_f(S-S_f)}{\mu_V(S_V-S)} \tag{1}$$

where λ_f is the annihilation rate in the defect free state; μ_V is the specific positron trapping rate into mono-vacancies. Because of the lattice structure and defects information is similar with pure Ni. Thus, the constant of Ni were chosen for our estimation (λ_f =9.1×10^{9} s^{-1}; μ_V =2.2×10^{15} s^{-1} [18]); S_f and S_V are the S parameters characteristic of the positron annihilation from matrix and mono-vacancy-trapped state, respectively. S_f = 0.435 and 0.437 for FeCrNi and Mo-diluted alloy, respectively. As reported, S_V in pure Ni is equal to the saturated S value of cold rolled specimen (more than 10%)[19]. The saturated S value in plastic deformed Fe17Cr14.5Ni alloy at room temperature is about 0.455±0.001. Thus, S_V =0.455 was chosen in the calculation. The defect concentration was calculated about 10^{-7} for both alloys at lower irradiation dose, while 10^{-4} for FeCrNi alloy and 10^{-6} for Mo-diluted alloy at elevated irradiation dose.

Usually, point defects might be trapped by solute atoms because of the attribution of the solid solution effect [20]. Meanwhile, the over-sized solute might reduce vacancy migration due to the high binding energy between the oversized atom and vacancy [16]. In the present study, the added Mo, as over-sized solute, existed in the alloy as solid solution state. The addition of Mo would trap vacancies and suppress the vacancy migration and growth. Therefore, swelling might be suppressed for the solid solution effect in Mo-diluted alloy.

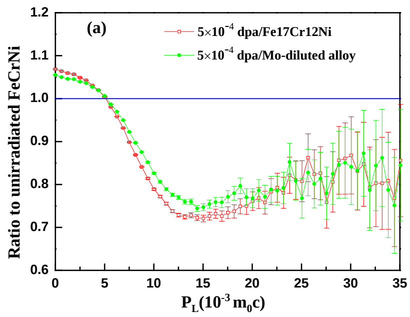

Figure 4 (a). Ratio curves of CDB spectra normalized to the momentum distribution of as-annealed FeCrNi alloy.

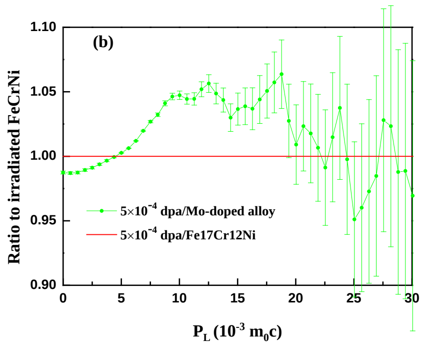

Figure 4 (b). Ratio curves of CDB spectra normalized to the momentum distribution of as-irradiated FeCrNi alloy.

CDB spectra could identify the chemical composition of the positron trapping site by measuring the momentum distribution of the electron annihilated with positron [15-16, 21-22]. As shown in Fig. 4, the CDB ratio curves of irradiated specimens were normalized to the momentum distribution of FeCrNi alloy. One peak within the momentum region of $8\times10^{-3}m_0c<|P_L|<18\times10^{-3}m_0c$ is observed in Fig. 4 (b). The solute Mo atoms might trap vacancies to form Mo-vacancy complex, which would change the chemical composition around vacancy sites compared to FeCrNi. Part of incident positrons, trapped by vacancies, annihilated with the characteristic core electron of Mo atoms. The effect of Mo-vacancy complex induced the generation of the peak at high-momentum region, as shown in Figure. 4 (b).

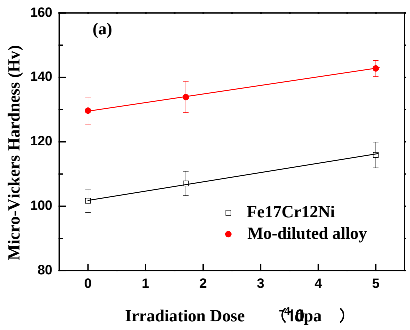

Figure 5 (a). Dose dependence of micro-Vickers Hardness plot for different model alloys.

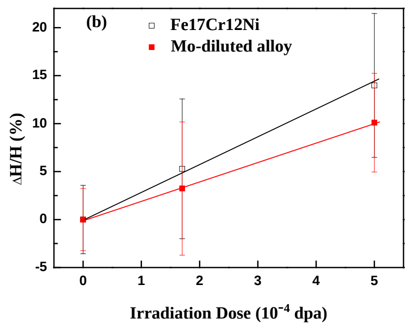

Figure 5 (b). ΔH/H parameters for both alloys at different radiation dose.

The hardness could be related with the microstructural features. The micro defects, such as dislocation loop, vacancy cluster or micro void, and precipitates could induce hardening in material [21, 23-24]. The micro-Vickers hardness value indicates that a significant difference exists between the two alloys, as shown in Fig. 5. The increment of hardness for both alloys attributed to the vacancy defects induced by electron irradiation. $\Delta H/H=(H_{irra}-H_{unirra})/H_{unirra}$, increased linearly for both alloy, as shown in Fig. 5 (b). The slope of FeCrNi is larger than that of the Mo-diluted alloy in Fig. 5 (b). Irradiation hardening could be suppressed because of the Mo addition, which is consistent with the defect concentration. Additionally, Mo-diluted alloy shows a considerable increase in hardness compared to the FeCrNi at the same irradiation condition, as shown in Fig. 5 (a). The solution strength induced by the added Mo atoms might be the main reason for this phenomenon [25-26].

4. Conclusion

PATs were performed to characterize the microstructural evolution in electron irradiated FeCrNi and Mo-diluted alloy as a function of dose dependence. The hardening process related with defect concentration was characterized by micro-Vickers Hardness. Certain amount of small-sized vacancies generated in the material after electron irradiation. The defect concentration was estimated about 10^{-4} for FeCrNi alloy and 10^{-6} for Mo-diluted alloy at elevated irradiation dose, while 10^{-7} for both alloys at lower dose. The diluted Mo could trap the vacancy defects to form Mo-vacancy complex and suppress the migration and growth of vacancy defects during electron irradiation. Hardening process was suppressed because of the Mo addition. Swelling would be suppressed in Mo-diluted FeCrNi austenitic alloy under irradiation.

5. Acknowledgements

This work is supported by the National Natural Science foundation of China 91226103 and 91026006.

References

[1] Yoshiie T，Sato K，Cao X，Xu Q，Horiki M，Troev T D 2012 *J. Nucl. Mater.* **429** 185-189

[2] Druzhkov A P，Perminov D A，Davletshin A E 2009 *J. Nucl. Mater.* **384** 56-60

[3] Garner F A 1984 *J. Nucl. Mater.* **122** 459-471

[4] Okita T，Kamada T，Sekimura N 2000 *J. Nucl. Mater.* **283** 220-223

[5] Okita T，Sato T，Sekimura N，Garner F A，Greenwood L R 2002 *J. Nucl. Mater.* **307** 322-326

[6] Brailsford A D，Bullough R 1982 *Cc/Eng Tech Appl Sci.* 22-22

[7] Yoshiie T，Cao X Z，Xu Q，Sato K，Troev T D 2009 *Phys Status Solidi* C. **6** 2333-2335

[8] Yoshiie T，Cao X Z，Sato K，Miyawaki K，Xu Q 2011 *J. Nucl. Mater.* **417** 968-971

[9] Horiki M，Yoshiie T，Huang S S，Sato K，Cao X Z，Xu Q，Troev T D 2013 *J. Nucl. Mater.* **442** S813-S816

[10] Shigenaka N，Hashimoto T，Fuse M 1993 *J. Nucl. Mater.* **207** 46-52

[11] LaSalvia J C，Kim D K，Meyers M A 1996 *Mat Sci Eng a-Struct.* **206** 71-80

[12] Pardo A，Merino M C，Coy A E，Viejo F，Arrabal R，Matykina E 2008 *Corros Sci.* **50** 780-794

[13] Shi F，Qi Y，Liu C M 2011 *J Mater Sci Technol.* **27** 1125-1130

[14] Chun Y B，Hwang S K，Kim M H，Kwun S I，Chae S W 2001 *J. Nucl. Mater.* **295** 31-41

[15] Nagai Y，Takadate K，Tang Z，Ohkubo H，Sunaga H，Takizawa H，Hasegawa M 2003 *Phys. Rev.* B. **67**

[16] AsokaKumar P，Alatalo M，Ghosh V J，Kruseman A C，Nielsen B，Lynn K G 1996 *Phys Rev Lett.* **77** 2097-2100

[17] Druzhkov A P，Perminov D A，Arbuzov V L 2013 *J. Nucl. Mater.* **434** 198-202

[18] Druzhkov A P，Perminov D A，Pecherkina N L 2008 *Philos Mag.* **88** 959-976

[19] Druzhkov A P，Arbuzov V L，Perminov D A 2012 *J. Nucl. Mater.* **421** 58-63

[20] Katoh Y，Kohyama A 1995 *Nucl Instrum Meth* B. **102** 12-18

[21] Nagai Y，Takadate K，Tang Z，Ohkubo H，Sunaga H，Takizawa H，Hasegawa M 2011 *International Workshop on Positron Studies of Defects (Psd 08).* **265**

[22] Hasegawa M，Nagai Y，Tang Z 2004 *32nd Course of the International School of Solid State Physics: Radiation Effects in Solids.* **July 19-28** P23

[23] Matsuoka H，Yamasaki T，Zheng Y J，Mitamura T，Terasawa M，Fukami T 2007 *Mat Sci Eng a-Struct.* **449** 790-793

[24] Liu X B，Wang R S，Jiang J，Wu Y C，Zhang C H，Ren A，Xu C L，Qian W J 2014 *J. Nucl. Mater.* **451** 249-254

[25] Tahir M I 1977 *Pak. J. Sci. Res.* **29** 39-45

[26] Franke O，Durst K，Goken M 2009 *J Mater Res.* **24** 1127-1134